02,11

Temperature and magnetic field dependences of the critical current in superconducting films of niobium nitride

© M.A. Vasyutin, N.D. Kuz'michev, D.A. Shilkin

Mordovia State University,
Saransk, Russia

E-mail: vasyutinm@mail.ru

Received April 24, 2024
Revised May 14, 2024 Accepted May 15, 2024

The current-voltage characteristics (C-V characteristics) of superconducting films of niobium nitride (NbN) were studied at temperatures below the transition temperature to the superconducting state (T_c) in a constant magnetic field. The temperature and magnetic field dependences of the critical film depinning current density (j_d) are determined. Within the framework of models of collective pinning and rigid pinning of vortices, functional dependences of j_d were found in the temperature range from $00.7T_c$ to $0.95T_c$ for magnetic fields with strengths up to 80 kOe. From the magnetic field dependences of j_d, confirmation of the presence of a region of constant critical current for the films under study in fields of $11-13$ kOe was obtained, which is explained by the existence of a regular structure of pinning centers in the samples. The distances between pinning centers and their sizes are estimated. The characteristic values of the vortex pinning force and the viscosity coefficient during their motion are determined.

Keywords: superconductors, niobium nitride, superconducting films, current-voltage characteristics.

DOI: 10.61011/PSS.2024.07.58985.102

1. Introduction

The studies of superconducting films of niobium nitride (NbN) are of high importance for both, the applied and fundamental sciences. The films of niobium nitride are simple in fabrication, chemical and radiation-resistant, have high mechanical strength and high second critical field. In applied physics they are used as single-photon detectors [1], resonant cavities for parametric amplifiers [2], energy accumulators [3], voltage standards [4] and etc. Recently the low-dimensional structures based on niobium nitride used as logical elements in cryogenic computers have been extensively studied [5]. Inverse spin-Hall effect [6], perspective for the spintronics was discovered in the niobium nitride.

The fundamental studies of niobium nitride are related, for example, with the study of superconductor-insulator junction in NbN ultra-fine films [7]. The discovery of Higgs mode in NbN samples was a crucial discovery in the elementary physics [8]. The study [9] has discovered a co-existence of a pseudo-slot and zero-dimensional fluctuations of the order parameter amplitude in the niobium nitride that can be explained by specific confinement of the superconducting fluctuations. A strong anisotropy of magnetization and critical currents was discovered in films equivalent to the studied ones [10].

The study of temperature and magnetic field dependences of critical current in NbN films is the continuation of papers [11–13], where the temperature dependence of the second critical magnetic field of these samples and other parameters were analyzed.

2. Theory

The critical current defined in this study based on the current-voltage curve (CVC) of samples is a structurally sensitive parameter of the superconductor, which shall be taken into account when analyzing its temperature and magnetic field dependencies. In the studied films the inhomogeneities which are the pinning centers, exist in the form of columnar grain boundaries and inter-granular defects. At that, the boundary area of several neighboring columns can more reliably fix the Abrikosov vortices compared to the stretched boundaries of two neighboring columns or inter-granular defects. This is due to the fact that coherence length ξ in the studied superconductor is close to the size of the inter-column area at temperatures near the temperature of transition into superconducting state T_c, while the distance between these areas is equal to the vortex lattice period in the magnetic field with intensity of ≈ 12 kOe.

Taking into account the availability of a quite thin ($1-2$ nm) dielectric interlayer between the granules [14], we may assume that in magnetic fields generating the cores of Abrikosov vortices with a size several times higher than the interlayer thickness, in NbN samples with high density of vacancies a mechanism of collective pinning may arise. This situation is possible only when the centers of strong pinning (with sizes close to the vortices cores) will be fully occupied and in higher fields the additionally occurring vortices will be fixed in finer heterogeneities (stretched inter-column layers and atomic size of the vacancies).

The collective pinning of single vortices significantly influences the density of de-pinning critical current j_d, at that the temperature dependence $j_d(T)$ is defined by the disordering parameter δ. In case of $\delta\ell$-pinning, when parameter δ is related to deviation of the free paths of the current carriers ℓ, its dependence from temperature T is defined by the expression [15]:

$$\delta\ell = 0.13 \cdot (1 - T/T_c)^{3/2}/(\xi_{BCS}\ell^2 n_i),$$

where $\xi_{BCS} = 0.18 \cdot \hbar v_F/(k_B T_c)$ — coherence length in BCS theory, $\hbar$ — Plank constant, v_F — electrons velocity of Fermi surface, k_B — Boltzmann constant, n_i — concentration of defects. De-pinning current density in our case

$$j_d = j_0 \delta^{2/3}, \tag{1}$$

where $j_0 = c\Phi_0/(12 \cdot 3^{1/2}\pi^2\lambda^2\xi)$ — density of scattering current, $c = 3 \cdot 10^{10}$ cm/c — light velocity, $\Phi_0 = 2.07 \cdot 10^{-7}\,\mathrm{G \cdot cm^2}$ — quantum of magnetic field, λ — London penetration depth of a magnetic field.

Then, for the de-pinning current density, taking into account the temperature dependencies λ and ξ, we may obtain [16]: $j_d \propto (1 - T/T_c)^{5/2}$.

The theory of a rigidly fixed vortex lattice may serve the model of strong pinning [17,18]. In this model the destruction of superconductivity by the impact of current, according to authors, is associated with reaching the superconducting critical velocity condensate. From the energy assumptions and linear approximation of the sample magnetization versus external magnetic field intensity H for the critical current density we may obtain j_c (at $H \gg H_{c1}$):

$$j_c = (cH_c/(4\pi\lambda))(1 - H/H_{c2})^2, \tag{2}$$

where H_c, H_{c1}, H_{c2} — intensities of thermodynamic, first and second critical magnetic fields, respectively.

In the studied current-voltage curves after a short non-linear section we may observe a linear dependence related to the motion of the vortex lattice as a whole. In this case, the resistivity of the flux in the magnetic field with inductance B and viscosity coefficient η is defined from the formula [19]:

$$\rho_f = \Phi_0 B/(c^2\eta). \tag{3}$$

A step-like voltage increase, observed after a linear section of current-voltage curve when the sample transits into normal state is associated with manifestation of Larkin–Ovchinnikov instability [20].

3. Experiment

This paper outlines the study of NbN films $d = 400-700$ nm thick, $w = 5$ mm wide, $a = 9$ mm long obtained by method of a getter reactive cathode sputtering of the niobium target in the glowing discharge (DC current) in the argon and nitrogen environment with sputtering on the polished fused quartz substrates [21,22]. The substrates temperature was $t_s = 700\,^\circ$C. The ultimate vacuum maintained in the system was $1.4 \cdot 10^{-4}$ Pa. Operating pressure during sputtering — 4–8 Pa. Mean discharge current — 150 mA. The samples had a structure of columnar granular type formations, perpendicular to the substrate, with columns diameter $\sim 50-100$ nm and inter-layer thickness between them $\sim 1-2$ nm [14,10]. The value of T_c samples changed within 16.2–16.5 K. The width of superconducting transition ≈ 0.1 K. Resistivity in the normal state near transition $\sim 400-1200\,\mu\Omega \cdot$ cm (current and potential contacts were formed across the entire width of the sample). Temperature measurement error didn't exceed $\Delta T = 0.01$ K. The study was performed by a four-contact method with additional resistivity of [23] with the sample exposure to pulse current increasing from zero to ≈ 0.7 A for 0.25 ms. The critical current was defined when ≈ 0.1 V voltage was reached. For more details see the measurements procedure in [13].

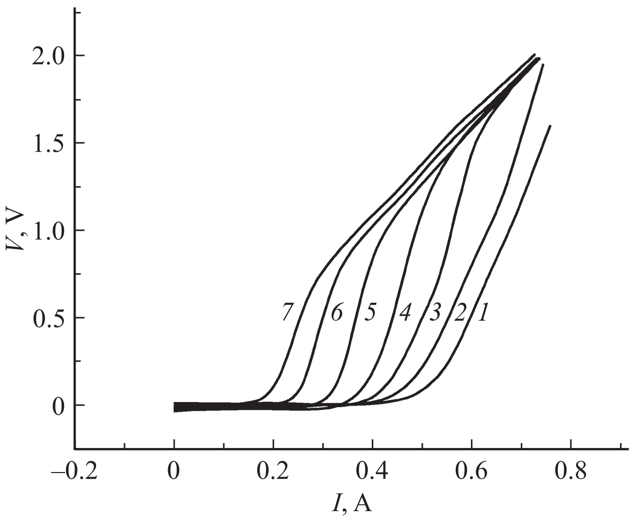

Figure 1. The current-voltage curves of NbN sample with $T_{c0} = 16.3$ K in a magnetic field with intensity of 10 kOe for the temperatures: *1* — 14.8 K, *2* — 14.9 K, *3* — 15 K, *4* — 15.1 K, *5* — 15.2 K, *6* — 15.3 K, *7* — 15.4 K.

Figure 1 illustrates the experimental current-voltage curves in NbN sample with $T_c = 16.3$ K at different temperatures in the constant field with intensity of $H = 10$ kOe. In the curve *3* we may identify four areas: initial non-linear slight growth of voltage followed by linear increase and a more sharp voltage jump transiting into a linear dependence when the normal state is established. These areas are less distinct or absent in the other curves. These dependencies were observed with values H from 5 to 80 kOe.

Figure 2 illustrates the current-voltage curves of the same sample in different magnetic fields at a temperature of 15.4 K. In the curves *1, 2, 3* we may see the characteristic parallel areas of linear increase $V(I)$ after a non-linear section; these areas are decreasing with a rate of H. Similar dependences are observed and for other temperatures in the range from 0.7 to $0.95T_c$.

By comparing Figure 1 and 2, we may see that the slope of curves in the jump area in Figure 2 is growing with a rate of H, while differential resistance of sample in this

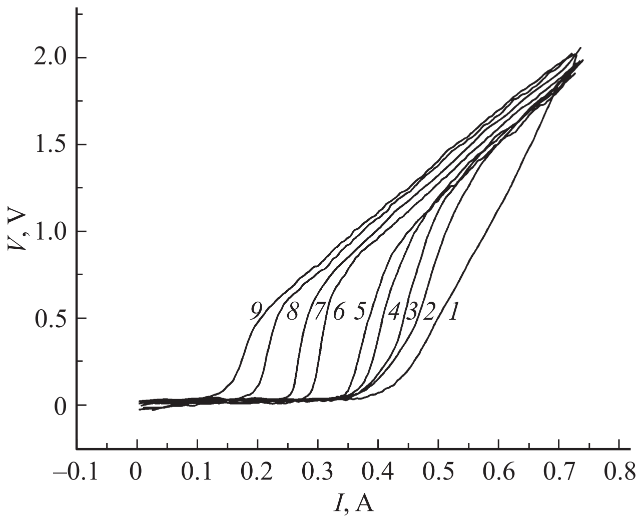

Figure 2. The current-voltage curves of NbN sample with $T_{c0} = 16.3\,\mathrm{K}$ at a temperature of 15.4 K in magnetic fields with intensity of: *1* — 0.5 kOe, *2* — 2.5 kOe, *3* — 3.75 kOe, *4* — 5 kOe, *5* — 6.25 kOe, *6* — 8.75 kOe, *7* — 10 kOe, *8* — 12.5 kOe, *9* — 15 kOe.

area of the CVC curve in Figure 1 doesn't depend on the temperature.

4. Processing of results and discussion

As known, the current density necessary for the breakage of Abrikosov vortex, fixed in the inhomogeneity with cross-sectional order and longer than coherence length, is close to the density of scattering current (see, for example, [19], page. 229). In our case, the characteristic densities of currents at the start of vortices motion are $\sim 10^4\,\mathrm{A/cm^2}$, while densities of the scattering currents for the corresponding temperatures are $\sim 10^6\,\mathrm{A/cm^2}$ [10]. Therefore, the model of a rigidly fixed vortex lattice is used in this study only for magnetic fields corresponding to the vortex lattice constant a_0, comparable with the distance between the neighboring pinning centers.

Given that H_c, H_{c2} and λ depend on the temperature, from the formula (2) we may get the temperature dependence of the de-pinning current density j_d in different magnetic fields [18]:

$$j_d(t) = j_c(0)\big[1 - H/H_{c2}(t)\big]^2(1 - t^2)^2, \qquad (4)$$

where $t = T/T_{c0}$ — reduced temperature, T_{c0} — superconducting temperature in zero magnetic field, $j_c(0) = (cH_c(0)/(4\pi\lambda(0)))$ — density of critical current at zero temperature in zero magnetic field.

By leaving unchanged the temperature portion of dependence $j_d(t)$, it is necessary to align the magnetic field dependence in formula (4) with the function $H_{c2}(t)$, consistent with our samples. The temperature dependence of the second critical magnetic field $H_{c2}(t)$ was obtained for our samples from WHH model and in the power function approximation was expressed by formula:

$$H_{c2}(t) = H_{c2}(0)(1 - t^6),$$

where $H_{c2}(0) = 137\,\mathrm{kOe}$ [11].

The insert window in Figure 3 illustrates experimental dependencies of de-pinning current density from the reduced temperature, models of rigidly fixed vortices approximated by $j_d(t)$ dependence (formula (4)). We can see that at temperatures$t = 0.93{-}0.95$ a sufficient inflection can be observed which is absent in the higher fields. This singularity can be explained by the increase of coherence length with the increase of temperature. Due to this, the diameters of Abrikosov vertices cores equal to the coherence length $(\xi = (\Phi_0/(2\pi H_{c2}(t)))^{1/2})$, are reaching the diameters of circles inscribed in the inter-columnar area (centers of pinning). In our case $\xi \approx 8\,\mathrm{nm}$.

The experimental data $j_d(T)$, shown in Figure 3 were approximated within collective pinning model by means of dependence (1) that for our samples in the magnetic field looks as follows:

$$j_d = j_0(0)\big(H^*/(H^* + H)\big)\big(1 - T/T_c(H)\big)^{5/2}, \qquad (5)$$

where $j_0(0) = 8.34 \cdot 10^6\,\mathrm{A/cm^2}$ — scattering current density of the studied samples at zero temperature in zero magnetic field, H^* — intensity of magnetic field peculiar to this sample $T_c(H)$ — superconducting transition temperature in a magnetic field with intensity of H. The figure shows that

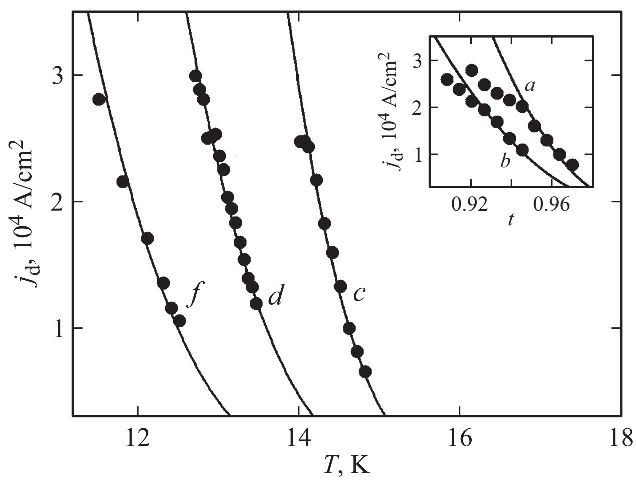

Figure 3. Experimental (black circles) and theoretical (solid lines, formula (5)) dependencies of de-pinning current of NbN sample with $T_{c0} = 16.3\,\mathrm{K}$ from the temperature for magnetic fields with intensity of H: c — $H = 30\,\mathrm{kOe}$, $H^* = 150\,\mathrm{kOe}$, $T_c(H = 30\,\mathrm{kOe}) = 15.77\,\mathrm{K}$; d — $H = 55\,\mathrm{kOe}$, $H^* = 34\,\mathrm{kOe}$, $T_c(H = 55\,\mathrm{kOe}) = 15.1\,\mathrm{K}$; f — $H = 80\,\mathrm{kOe}$, $H^* = 24\,\mathrm{kOe}$, $T_c(H = 80\,\mathrm{kOe}) = 14.2\,\mathrm{K}$. The insert window in the Figure shows equivalent experimental dependencies, approximated by formula (4): a — $H = 5\,\mathrm{kOe}$, $j_c(0) = 2.2 \cdot 10^6\,\mathrm{A/cm^2}$; b — $H = 10\,\mathrm{kOe}$, $j_c(0) = 1.25 \cdot 10^6\,\mathrm{A/cm^2}$; The measurement error is equal to the circle diameter.

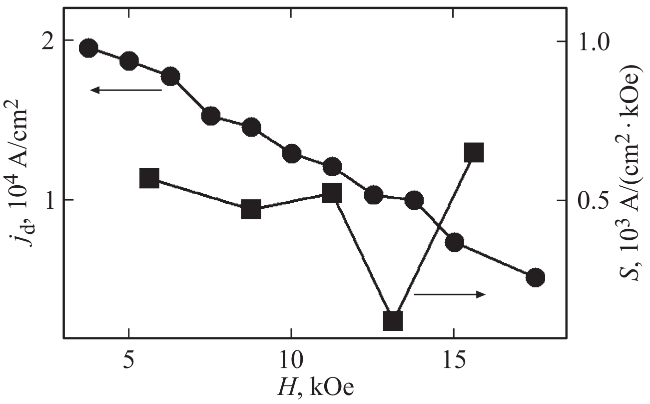

Figure 4. Experimental dependencies of the critical de-pinning current density j_d of NbN sample with $T_c = 16.3$ K from H magnetic field at a temperature of $T = 15.4$ K (circles). Derivative j_d with respect to $H(S = -(dj_d/dH)$, squares). The measurement error is equal to the circle diameter.

the theory and the experiment are consistent with each other at $j_d \propto H^{-1}$.

Figure 4 illustrates the critical de-pinning current density versus applied magnetic field $j_d(H)$ at a temperature of $T = 15.4$ K. The figure also shows the calculated averaged derivative j_d with respect to $H(S = -(d_{j_d}/dH))$. We see that in the field with intensity of 12−14 kOe $j_d(H)$ is practically unchanged, which can be explained by coincidence of distances between the nearest pinning centers (model domains between the three neighboring contacting granular columns) with distances between the Abrikosov vortices cores at a given magnetic field. Moreover, with temperatures $t = 0.92{-}0.94$, as in case of inflections shown in Figure 3, a general dependence of pinning enhancement is observed when the sizes of Abrikosov vortices cores and pinning centers coincide.

Analyzing the inter-vortex distance by formula: $a_0 = (\Phi_0/B)^{1/2}$, we may get (at $B = 1.3 \cdot 10^4$ G) $a = 4 \cdot 10^{-6}$ cm = 40 nm. This corresponds to the diameter of granules $d = a/(\mathrm{tg}\,30^\circ) = a \cdot \sqrt{3} \approx 70$ nm, which is in line with their average diameter [14].

The linear portion of current-voltage curve of the studied samples can be explained by the flux model (linear dependence V from I in Figure 1 and in Figure 2 in curves *1, 2, 3*). Using formula (3) we may estimate the viscosity of environment where vortices are moving (in SI system): $\eta = \Phi_0 B/(\rho_f)$. For $B = 0.25$ T and resistivity $\rho_f \approx 4 \cdot 10^{-6}\,\Omega \cdot$ m we'll obtain $\eta \approx 1.3 \cdot 10^{-10}\,\mathrm{T}^2 \cdot \mathrm{m}/\Omega$.

We may judge about the vortices pinning force at certain temperatures by observing the initial motion of the vortex lattice. Figure 1 for the curve *2* shows the current corresponding to the start of the linear section, $I \approx 0.5$ A. Density of current $j \approx 2.5 \cdot 10^4$ A/cm^2. Then, the mean pinning forth per unit vortex length can be found from the formula (in SI system): $f = j\Phi_0$. For this j we'll obtain $f \approx 5.2 \cdot 10^{-7}$ N/m.

The decrease of the linear portion of the current-voltage curve, associated with the flux (curves *1, 2, 3* in Figure 2), can be explained by the higher number of vortices in the sample with the field growth. With the field intensity approaching ≈ 12 kOe, when the number of vortices becomes equal to the number of strong pinning centers the shift of the entire vortex lattice requires a strong force. And this, in its turn, causes a more quick occurrence of Larkin-Ovchinnikov instability.

The flux defined by the linear dependence $V(I)$ in curve *1* Figure 1 and 2, covers almost the whole transition and practically defines the sample transfer to normal state that could be explained by the shortage of the current carriers ([19], p. 96). The Larkin-Ovchinnikov instability is absent.

5. Conclusion

The temperature and magnetic field dependencies of critical current for NbN films transition to normal state, studied in this paper, are depending on pinning and motion of Abrikosov vortices in case of their viscous flux. This study describes the values of the scattering current density $j_0(0)$ for the single-vortex collective pinning, the characteristic dimensions of the pinning centers and distance between them. The viscosity coefficient and pinning force were calculated. The obtained parameters and temperature and magnetic field dependencies of critical current could be useful, e.g., in development of energy accumulators [3], where the films with thickness close to the studied ones are used. Such films could be used also as magnetic field sensors in the magnetometers [24].

Conflict of interest

The authors declare that they have no conflict of interest.

References

[1] R. Yin, H. Wang, L. Zhang, X. Wang, L. Ma, Y. Guan, Z. Yang, Q. Chen, X. Tu, Q. Zhao, X. Jia, J. Chen, L. Kang, P. Wu. Supercond. Sci. Technol. **36**, *10*, 105016 (2023). DOI: 10.1088/1361-6668/acf5aa

[2] S. Zhao, S. Withington, C.N. Thomas. Supercond. Sci. Technol. **36**, *10*, 105010 (2023). DOI: 10.1088/1361-6668/acf0f1

[3] Y. Suzuki, N. Iguchi, K. Adachi, A. Ichiki, T. Hioki, C.-W. Hsu, R. Sato, S. Kumagai, M. Sasaki, J.-H. Noh, Y. Sakurahara, K. Okabe, O. Takai, H. Honma, H. Watanabe, H. Sakoda, H. Sasagawa, H. Doy, S. Zhou, H. Hori, S. Nishikawa, T. Nozaki, N. Sugimoto, T. Motohiro. J. Phys.: Conf. Ser. **897**, *1*, 012019 (2017). DOI: 10.1088/1742-6596/897/1/012019

[4] S. Solve, R. Chayramy, M. Maruyama, C. Urano, N.-H. Kaneko, A. Rüfenacht. Metrologia. **55**, *2*, 302 (2018). DOI: 10.1088/1681-7575/aaac44

[5] B.A. Gurovich, K.E. Prikhodko, L.V. Kutuzov, B.V. Goncharov, D.A. Komarov, E.M. Malieva, G.Yu. Golubev. FTT **65**, *7*, 1118 (2023). (in Russian). DOI: 10.21883/FTT.2023.07.55831.24H

[6] T. Wakamura, H. Akaike, Y. Omori, Y. Niimi, S. Takahashi, A. Fujimaki, S. Maekawa, Y. Otani. Nature Mater. **14**, 675 (2015).
[7] J. Yong T.R. Lemberger, L. Benfatto, K. Ilin, M. Siegel. Phys. Rev. B **87**, 184505 (2013).
[8] D. Sherman, U.S. Pracht, B. Gorshunov, S. Poran, J. Jesudasan, M. Chand, P. Raychaudhuri, M. Swanson, N. Trivedi, A. Auerbach, M. Scheffler, A. Frydman, M. Dressel. Nature Phys. **11**, 188 (2015).
[9] C. Carbillet, S. Caprara, M. Grilli, C. Brun, T. Cren, F. Debontridder, B. Vignolle, W. Tabis, D. Demaille, L. Largeau, K. Ilin, M. Siegel, D. Roditchev, B. Leridon. Phys. Rev. B **93**, 144509 (2016).
[10] D.M. Gokhfeld, N.E. Savitskaya, S.I. Popkov, N.D. Kuzmichev, M.A. Vasyutin, D.A. Balaev. ZhETF **161**, *6*, 833 (2022). (in Russian). DOI: 10.31857/S0044451022060062
[11] M.A. Vasyutin, N.D. Kuzmichev, D.A. Shilkin. FTT **58**, *2*, 231 (2016). (in Russian).
[12] M.A. Vasyutin, N.D. Kuzmichev, D.A. Shilkin. FTT **60**, *11*, 2247 (2018). (in Russian).
[13] M.A. Vasyutin, N.D. Kuzmichev, D.A. Shilkin. FMM **121**, *10*, 1045 (2020). (in Russian).
[14] E.A. Antonova, V.A. Sukhov. FNT **7**, *8*, 1002 (1981). (in Russian).
[15] G. Blatter, M.V. Feigelman, V.G. Geshkenbein, A.I. Larkin, V.M. Vinokur. Rev. Mod. Phys. **66**, *4*, 1125 (1994).
[16] E.A. Pashitsky, V.I. Vakaruyk, S.M. Ryabchenko, Yu.V. Fedotov. FNT **27**, *2*, 131 (2001). (in Russian).
[17] Yu.F. Bychkov, V.G. Vereschagin, V.R. Karasik, G.B. Kurganov, V.A. Mal'tsev. ZhETF **56**, *2*, 505 (1969). (in Russian).
[18] Yu.F. Bychkov, V.G. Vereschagin, M.T. Zuev, V.R. Karasik, G.B. Kurganov, V.A. Mal'tsev. Pis'ma v ZhETF **9**, *8*, 451 (1969). (in Russian).
[19] V.V. Schmidt. Vvedenie v fiziku sverkhprovodnikov. Ed. 3rd edition. MTsNMO, M (2000). XIV. 402 p. (in Russian).
[20] A.I. Larkin, Yu.N. Ovchinnikov. ZhETF **68**, *5*, 1915 (1975). (in Russian).
[21] N.D. Kuzmichev, G.P. Motulevitch. ZhETF **84**, *6*, 2316 (1983). (in Russian).
[22] D.R. Juraev, G.P. Motulevitch. FTT **27**, *9*, 2640 (1985). (in Russian).
[23] M.A. Vasyutin, N.D. Kuzmichev, D.A. Shilkin. Pisma v ZhTF **48**, *14*, 34 (2022). (in Russian). DOI: 10.21883/PJTF.2022.14.52868.19131
[24] N.D. Kuzmichev, M.A. Vasyutin, D.A. Shilkin. Prikladnaya fizika, **4**, *92* (2020) (in Russian).

Translated by T.Zorina